

Effect of π -linkers on Phenothiazine Sensitizers for Dye-Sensitized Solar Cells

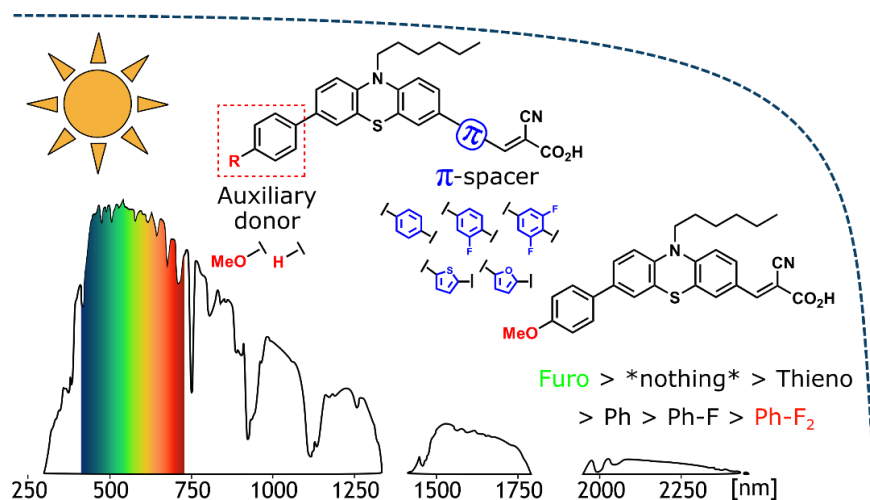
Audun Formo Buene, Nora Uggerud, Solon P. Economopoulos, Odd R. Gautun, Bård Helge Hoff*

Department of Chemistry, Norwegian University of Science and Technology, Høgskoleringen 5, NO-7491 Trondheim, Norway

* Corresponding author. Tel.: +47 73593973; E-mail address: bard.helge.hoff@chem.ntnu.no (B. H. Hoff).

Abstract

Eleven new dyes have been synthesized in order to investigate the effect of five different π -spacers and two different auxiliary donors in phenothiazine-based sensitizers for dye-sensitized solar cells. The target molecules were synthesized in 5 to 7 steps from 10*H*-phenothiazine. Evaluation of the photovoltaic performance revealed that introducing a π -spacer does not necessarily increase the power conversion efficiency. Still, dyes with a furan π -spacer were found to be slightly more efficient compared to their thiophene counterparts, and more efficient than no spacer. Dyes with phenyl based π -spacers resulted in less efficient solar cells, and especially so when incorporating two fluorine atoms. Surprisingly, introducing an additional electron donating group in the auxiliary donor had no pronounced effect on the photovoltaic performance of the dyes.



Keywords: Phenothiazine dyes, Dye-sensitized solar cells, π -spacer, Auxiliary donor, Furan

1 Introduction

The need for increasing global power production has sparked the development of a number of new photovoltaic technologies. Dye-sensitized solar cells (DSSCs) are promising candidates allowing solar cells to be semi-transparent, flexible and of tunable color. [1] Under ambient light conditions, DSSCs have outperformed most other long established PV technologies. [2] Hot applications of DSSCs include building integration and powering an increasing number of devices in the Internet of Things (IoT). [3] This development has, to a large extent, been supported by the introduction of new redox shuttles based on cobalt and copper complexes. [4-8]

The dyes utilized in DSSCs have traditionally been metal-complexes, where N719, N3 and N749 also known as 'black dye' are the most famous examples. [9] Zinc porphyrins are also highly successful sensitizers with a metal-organic core. [10] In terms of efficiency, these metal-based complexes have achieved PCEs up to 13.0 % [11]. Although the absorption properties of these dyes are excellent, the extinction coefficients are usually moderate and dye aggregation, synthesis and purification are common challenges. Thus, metal-free dyes have emerged as a viable alternative. [12]

Improving the stability and efficiency of metal-free dyes is where the main efforts in this research area have been placed, and the current record for metal-free dyes is 14.7%. [8] Triarylamines, phenothiazines and polythiophenes are common dye scaffolds. [13, 14] Phenothiazine, and its oxygen analog phenoxazine, were among the early metal-free dyes, and studies of π -spacers containing isomerizable double bonds have been conducted. [15, 16] Furthermore, this class of sensitizers have shown very promising results in DSSCs with aqueous electrolytes, as demonstrated by Lin et al. [17] The phenothiazine dye scaffold has been the subject of two recent reviews for the interested reader, and as with any other class of dyes the main challenge lies in improving the light harvesting properties of the molecules. [18, 19] Pushing the absorption towards the infrared region of the spectrum is crucial, and the introduction of π -spacers and auxiliary donors can be efficient measures for achieving this.

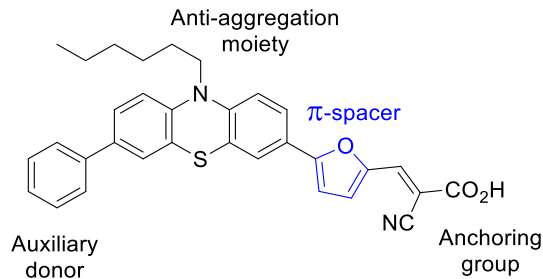


Figure 1. General layout of the sensitizers in this study, illustrated by **AFB-10**.

While several studies have investigated the effect of different π -spacers [20-24], the lack of a larger data set is apparent. A study comparing five and six-membered π -spacers directly connecting the phenothiazine scaffold and anchoring group has to the best of our knowledge only been performed by Bodedla et al. comparing thiophene and phenyl. [24] They reported an insulating behavior of the phenyl spacer due to non-planarity, reducing the interactions between the donor and acceptor moieties. We prepared two complementary series of dyes with the same five π -spacers, to observe and verify any appearing trends. The two series of dyes only differ by the auxiliary donor group on the phenothiazine scaffold, and one of the series was extended with a reference dye without any π -spacer. The general layout of the sensitizers is illustrated by **AFB-10** in Figure 1.

2 Experimental section

2.1 Materials and reagents

All reactions were carried out under nitrogen atmosphere, and all synthesis reagents were acquired from Sigma Aldrich.

2.2 Analytical instruments

¹H and ¹³C NMR spectra were recorded at 22 °C on either a Bruker 400 or 600 MHz spectrometer in DMSO-*d*₆. All chemical shifts are reported in ppm, and the spectra were calibrated using the signal of DMSO at 2.50 ppm (¹H) and 39.52 (¹³C), or that of of TMS (0 ppm) in CDCl₃. Infrared absorption (IR) spectra were recorded with a FTIR Thermo Nicolet Nexus FT-IR Spectrometer using a Smart Endurance reflection cell.

Reported frequencies were in the range of 4000-400 cm^{-1} . UV/Vis analyses were performed with a Hitachi U-1900 UV/Vis-spectrophotometer using quartz cuvettes (10 mm). Extinction coefficients were calculated from Lambert-Beer's law. UV/Vis measurements of sensitized TiO_2 films was performed in the same spectrophotometer with a non-stained electrode as the background. Melting points were determined with a Stuart SMP40 automatic melting point instrument. Accurate mass determination in positive and negative mode was performed on a "Synapt G2-S" Q-TOF instrument from WatersTM. The samples were ionized by the use of ASAP probe (APCI) or by ESI. Spectra processing was done by WatersTM Software (Masslynx v4.1 SCN871). Fluorescence spectrophotometry was carried out on a Varian Cary Eclipse instrument. All emission spectra were measured in chloroform.

2.3 Fabrication of dye-sensitized solar cells

The cell fabrication is conducted based on the procedure from Hao et al. [25] TEC-8 FTO glass supplied by Dyesol was washed with Deconex 21 (2 g/L H_2O) in an ultrasonic bath for 45 minutes, and then rinsed with deionized water and ethanol before air drying. Further cleaning was done in a UV-ozone cleaner for 15 minutes (Novascan PSD PRO-UV T6). A blocking layer was deposited by immersion of the FTO glass in an aq. solution of TiCl_4 (40 mM) for 30 minutes at 70 °C, rinsing with deionized water and ethanol followed by another immersion for 30 minutes in an aq. solution of TiCl_4 (40 mM) at 70 °C, then rinsing with deionized water and ethanol.

Five layers of transparent TiO_2 paste (18NR-T, Dyesol) were screen printed on the FTO glass (mesh count 250, active area 0.238 cm^2). Between each layer, the electrodes were heated to 125 °C for 2-3 minutes. Finally, a scattering layer (WER2-O, Dyesol) was screen printed, and the electrodes were sintered at 500 °C for 30 minutes. The thickness of the sintered TiO_2 was measured to 17.5 μm (12.5 μm + 5 μm) with a profilometer (Veeco, Dektak 150). The electrodes were then post treated with TiCl_4 using the same conditions previously described for 30 minutes.

Counter electrodes were fabricated by drilling holes in the FTO glass with a diamond drill bit. The catalytic Pt layer was deposited by dropcasting a 10 mM solution of H_2PtCl_6 in 2-propanol ($5 \mu\text{L}/\text{cm}^2$), followed by firing at $400 \text{ }^\circ\text{C}$ for 15 minutes. [6]

Before staining, the electrodes were annealed with a hot air gun at $480 \text{ }^\circ\text{C}$ for 25 minutes. The staining solution had $5 \times 10^{-4} \text{ M}$ dye concentration, with a 10-fold amount of CDCA in a mixture of acetonitrile/THF (43:57, v/v). The dielectric constant for this solution is estimated to be around 20 Fm^{-1} , which for Black dye is reported as the optimal dielectric constant. [26] N719 was stained from a 0.5 mM solution in ethanol. The electrodes were stained for 20 hours, then rinsed in acetonitrile for 2 minutes and dried under N_2 flow. The cells were sealed with a $25 \mu\text{m}$ Surlyn (Solaronix) gasket, melted with a 50 W PTC heat element for 3×20 seconds per cell.

The electrolyte was made following a procedure from Demadrille et al. [27], containing 0.5 M 1-butyl-3-methylimidazolium iodide, 0.1 M lithium iodide, 0.05 M I_2 and 0.5 M *tert*-butylpyridine in acetonitrile. This was injected by vacuum backfilling before the filling hole was sealed with Surlyn and a circular glass cover slip. The contacts for the anode and cathode were painted with a conductive silver paint (Electrolube, SCP) before characterization.

2.4 Device characterization

The device's I-V characteristics were measured with a Keithley 2450 under a Sciencetech SP300B solar simulator with an AM 1.5 G filter, calibrated to $100 \text{ mW}/\text{cm}^2$ with a Newport Reference Solar Cell and Meter (91150V). All cells were masked with a 0.1547 cm^2 black mask before characterization.

IPCE measurements were obtained from a device fabricated with a halogen lamp (Ocean Optics HL-2000), a monochromator (Spectral Products CM110), connected to the Keithley 2450. The light intensity was determined using a NIST traceable calibrated photodiode (Thorlabs, FDS100-CAL).

2.5 Synthesis

2.5.1 (E)-2-Cyano-3-(10-hexyl-7-(4-methoxyphenyl)-10H-phenothiazin-3-yl)acrylic acid (AFB-1)

Compound **5** (200 mg, 0.479 mmol) and cyanoacetic acid (815 mg, 9.58 mmol) were dissolved in degassed acetonitrile (55 mL) under N₂ atmosphere. Piperidine (569 μ L, 489 mg, 5.75 mmol) was added and the reaction was heated at 80 °C for 40 minutes before cooling to 22 °C and quenched in aqueous HCl (2 M, 150 mL). EtOAc (50 mL) was added and the organic phase was washed with water (8 \times 100 mL), then dried with brine (50 mL) and over anhydrous Na₂SO₄, filtered and the solvents were removed in vacuo. The crude product was purified by silica-gel column chromatography (gradient: 0-15% MeOH in CH₂Cl₂) to obtain **AFB-1** as a dark solid (215 mg, 0.444 mmol, 93%), mp. 204-208 °C. ¹H NMR (600 MHz, DMSO-*d*₆) δ : 13.72 (s, 1H), 8.15 (s, 1H), 7.91 (d, *J* = 8.8 Hz, 1H), 7.82 (s, 1H), 7.57 (d, *J* = 8.7 Hz, 2H), 7.45 (d, *J* = 8.6 Hz, 1H), 7.39 (s, 1H), 7.15 (d, *J* = 8.8 Hz, 1H), 7.09 (d, *J* = 8.6 Hz, 1H), 6.98 (d, *J* = 8.8 Hz, 2H), 3.94 (t, *J* = 7.0 Hz, 2H), 3.78 (s, 3H), 1.74-1.64 (m, 2H), 1.45-1.35 (m, 2H), 1.31-1.20 (m, 4H), 0.82 (t, *J* = 7.1 Hz, 3H); ¹³C NMR (150 MHz, DMSO-*d*₆) δ : 163.8, 158.8, 152.5, 148.6, 141.1, 135.3, 131.7, 130.9, 129.1, 127.2 (2C), 125.5, 125.4, 124.6, 122.7, 122.5, 116.8, 116.7, 115.5, 114.3 (2C), 99.4, 55.1, 47.0, 30.8, 26.0, 25.7, 22.1, 13.8; IR (neat, cm⁻¹) ν : 2909 (w), 1683 (m), 1558 (m), 1470 (s), 1184 (s), 826 (m); HRMS (ASAP+, *m/z*): 484.1815 (calcd. C₂₉H₂₈N₂O₃S: 484.1821 [M]⁺); UV (CH₂Cl₂, 2 \times 10⁻⁵ M, 22 °C) λ _{max} (nm): 305.5 (26200), 475.0 (14000).

2.5.2 (E)-2-Cyano-3-(4-(10-hexyl-7-phenyl-10H-phenothiazin-3-yl)phenyl)acrylic acid (AFB-2)

Dye **AFB-2** was made as described in Section 2.5.1 but starting with compound **10** (294 mg, 0.634 mmol), cyanoacetic acid (1.08 g, 12.7 mmol) and piperidine (753 μ L, 648.0 mg, 7.61 mmol). The crude product was purified by silica-gel column chromatography (gradient: 0-15% MeOH in CH₂Cl₂) to obtain **AFB-2** as a dark brown solid (164 mg, 0.308 mmol, 49%), mp. 246 °C (dec.). ¹H NMR (400 MHz, DMSO-*d*₆) δ : 8.05 (s, 1H), 7.95 (d, *J* = 8.4 Hz, 2H), 7.79 (d, *J* = 8.4 Hz, 2H), 7.65-7.61 (m, 2H), 7.59 (dd, *J* = 8.5 Hz, 2.1, 1H), 7.55 (d, *J* = 2.3 Hz, 1H), 7.50 (dd, *J* = 8.5, 2.3 Hz, 1H), 7.46 (d, *J* = 2.3 Hz, 1H), 7.44-7.40 (m, 2H),

7.32 (t, $J = 7.3$ Hz, 1H), 7.09 (dd, $J = 8.7, 2.1$ Hz, 2H), 3.92 (t, $J = 6.9$ Hz, 2H), 1.74-1.68 (m, 2H), 1.44-1.38 (m, 2H), 1.28-1.23 (m, 4H), 0.85-0.81 (m, 3H) (carboxylic acid proton not visible); ^{13}C NMR (100 MHz, $\text{DMSO-}d_6$) δ : 163.4, 147.9, 144.4, 143.5, 141.2, 138.8, 134.5, 132.9, 131.6, 130.2 (2C), 128.9 (2C), 127.1, 126.3 (2C), 126.1, 126.0 (2C), 125.9, 125.1, 125.0, 123.7, 123.5, 118.9, 116.1, 116.0, 111.4, 46.6, 30.8, 26.2, 25.8, 22.1, 13.8; IR (neat, cm^{-1}) ν : 2961 (w), 2925 (w), 2852 (w), 2218 (w), 1600 (m), 1579 (m), 1464 (m), 1393 (m), 1247 (m), 1189 (m), 808 (m), 758 (s), 696 (m); HRMS (ASAP+, m/z): 486.2127 (calcd. $\text{C}_{33}\text{H}_{30}\text{N}_2\text{S}$: 486.2130, $[\text{M-CO}_2+\text{H}]^+$); UV (CH_2Cl_2 , 2×10^{-5} M, 22 °C) λ_{max} (nm): 425.0 (11350).

2.5.3 (E)-2-Cyano-3-(4-(10-hexyl-7-(4-methoxyphenyl)-10H-phenothiazin-3-yl)phenyl)acrylic acid

(AFB-3)

Dye **AFB-3** was made as described in Section 2.5.1 but starting with compound **11** (190 mg, 0.385 mmol), cyanoacetic acid (655 mg, 7.70 mmol) and piperidine (457 μL , 393 mg, 4.62 mmol). The crude product was purified by silica-gel column chromatography (gradient: 0-15% MeOH in CH_2Cl_2) to obtain **AFB-3** as a dark brown solid (186 mg, 0.331 mmol, 86%), mp. 237 °C (dec.). ^1H NMR (400 MHz, $\text{DMSO-}d_6$) δ : 8.03 (s, 1H), 7.97-7.93 (m, 2H), 7.80-7.76 (m, 2H), 7.60-7.53 (m, 4H), 7.46-7.42 (m, 1H), 7.41-7.39 (m, 1H), 7.10-7.03 (m, 2H), 7.00-6.96 (m, 2H), 3.91 (t, $J = 6.9$ Hz, 2H), 3.78 (s, 3H), 1.76-1.66 (m, 2H), 1.45-1.36 (m, 2H), 1.29-1.21 (m, 4H), 0.86-0.80 (m, 3H) (carboxylic acid proton not visible); ^{13}C NMR (100 MHz, $\text{DMSO-}d_6$) δ : 163.2, 158.7, 147.9, 144.5, 142.8, 141.2, 134.3, 132.8, 131.6, 131.3, 130.2 (2C), 127.2 (2C), 126.3 (2C), 126.1, 125.3, 125.0, 124.5, 123.8, 123.5, 119.0, 116.1, 116.0, 114.3 (2C), 111.0, 55.2, 46.6, 30.9, 26.2, 25.8, 22.1, 13.8; IR (neat, cm^{-1}) ν : 3033 (w, br), 2925 (w), 2847 (w), 2223 (w), 1719 (m), 1693 (m), 1574 (s, br), 1460 (s), 1242 (s), 1179 (s), 1023 (m), 805 (s); HRMS (ASAP+, m/z): 516.2228 (calcd. $\text{C}_{34}\text{H}_{32}\text{N}_2\text{O}_2\text{S}$: 516.2235 $[\text{M-CO}_2]^+$); UV (CH_2Cl_2 , 2×10^{-5} M, 22 °C) λ_{max} (nm): 429.5 (12700).

2.5.4 (E)-2-Cyano-3-(2-fluoro-4-(10-hexyl-7-phenyl-10H-phenothiazin-3-yl)phenyl)acrylic acid (AFB-4)

Dye **AFB-4** was made as described in Section 2.5.1 but starting with compound **12** (205 mg, 0.425 mmol), cyanoacetic acid (722 mg, 8.49 mmol) and piperidine (504 μ L, 434 mg, 5.10 mmol). The crude product was purified by silica-gel column chromatography (gradient: 0-15% MeOH in CH_2Cl_2) to obtain **AFB-4** as a dark red solid (200 mg, 0.365 mmol, 86%), mp. 214 $^\circ\text{C}$ (dec.). ^1H NMR (400 MHz, $\text{DMSO-}d_6$) δ : 8.19 (t, $J = 8.2$ Hz, 1H), 8.14 (s, 1H), 7.70-7.57 (m, 6H), 7.53-7.48 (m, 1H), 7.47-7.39 (m, 3H), 7.35-7.29 (m, 1H), 7.12-7.05 (m, 2H), 3.92 (t, $J = 6.9$ Hz, 2H), 1.76-1.66 (m, 2H), 1.45-1.36 (m, 2H), 1.29-1.21 (m, 4H), 0.86-0.80 (m, 3H) (carboxylic acid proton not visible); ^{13}C NMR (100 MHz, $\text{DMSO-}d_6$) δ : 162.4, 160.9 (d, $J = 251$ Hz), 144.9, 143.5 (d, $J = 10.7$ Hz), 143.35, 138.8, 134.6, 131.8 (d, $J = 3.8$ Hz), 131.7, 130.2, 128.9 (2C), 128.6 (d, $J = 2.0$ Hz), 127.1, 126.2, 126.1 (2C), 125.9, 125.2, 125.0, 123.7, 123.4, 122.1 (d, $J = 2.1$ Hz), 119.3 (d, $J = 12.0$ Hz), 118.5, 116.0 (d, $J = 21.3$ Hz), 113.0, 112.7, 46.6, 30.8, 26.1, 25.8, 22.1, 13.8; IR (neat, cm^{-1}) ν : 2951 (w), 2935 (w), 2862 (w), 2218 (w), 1579 (m), 1465 (s), 1393 (m), 1257 (m), 808 (m), 758 (s), 696 (m); HRMS (ASAP+, m/z): 504.2035 (calcd. $\text{C}_{33}\text{H}_{29}\text{FN}_2\text{S}$: 505.2035, $[\text{M-CO}_2]^+$); UV (CH_2Cl_2 , 2×10^{-5} M, 22 $^\circ\text{C}$) λ_{max} (nm): 431.5 (12950).

2.5.5 (E)-2-Cyano-3-(2-fluoro-4-(10-hexyl-7-(4-methoxyphenyl)-10H-phenothiazin-3-yl)phenyl)acrylic acid (AFB-5)

Dye **AFB-5** was made as described in Section 2.5.1 but starting with compound **13** (186 mg, 0.364 mmol), cyanoacetic acid (618 mg, 7.27 mmol) and piperidine (432 μ L, 371 mg, 4.36 mmol). The crude product was purified by silica-gel column chromatography (gradient: 0-15% MeOH in CH_2Cl_2) to obtain **AFB-5** as a dark red solid (121 mg, 0.209 mmol, 58%), mp. 220 $^\circ\text{C}$ (dec.). ^1H NMR (400 MHz, $\text{DMSO-}d_6$) δ : 8.18 (t, $J = 8.0$ Hz, 1H), 8.12 (s, 1H), 7.70-7.65 (m, 2H), 7.63 (dd, $J = 8.5$ Hz, 2.2, 1H), 7.60-7.55 (m, 3H), 7.45 (dd, $J = 8.5, 2.1$ Hz, 1H), 7.40 (d, $J = 2.2$ Hz, 1H), 7.07 (t, $J = 8.4$ Hz, 2H), 6.98 (d, $J = 8.8$ Hz, 2H), 3.91 (t, $J = 6.9$ Hz, 2H), 3.78 (s, 3H), 1.75-1.67 (m, 2H), 1.45-1.36 (m, 2H), 1.30-1.21 (m, 4H), 0.86-0.81 (m,

3H) (carboxylic acid proton not visible); ^{13}C NMR (100 MHz, $\text{DMSO-}d_6$) δ : 162.4, 160.8 (d, $J = 251.1$ Hz), 158.7, 145.0, 143.4 (d, $J = 9.6$ Hz), 142.7, 138.3, 134.4, 131.6, 131.2, 128.5, 127.2 (2C), 126.2, 125.4, 125.1, 124.5, 123.7, 123.4, 122.1 (d, $J = 2.3$ Hz), 119.4 (d, $J = 11.5$ Hz), 118.7, 116.1, 115.8, 114.3 (2C), 112.9, 112.8, 55.2, 46.6, 30.8, 26.2, 25.8, 22.1, 13.8; IR (neat, cm^{-1}) ν : 3034 (w, br), 2925 (w), 2847 (w), 2223 (w), 1719 (m), 1693 (m), 1574 (s, br), 1460 (s), 1242 (s), 1179 (s), 1023 (m), 805 (s); HRMS (ASAP+, m/z): 534.2139 (calcd. $\text{C}_{34}\text{H}_{31}\text{N}_2\text{OFS}$: 534.2141 [M-CO_2] $^+$); UV (CH_2Cl_2 , 2×10^{-5} M, 22 °C) λ_{max} (nm): 440.5 (12050).

2.5.6 (E)-2-Cyano-3-(2,6-difluoro-4-(10-hexyl-7-phenyl-10H-phenothiazin-3-yl)phenyl)acrylic acid (AFB-6)

Dye **AFB-6** was made as described in Section 2.5.1 but starting with compound **14** (228 mg, 0.457 mmol), cyanoacetic acid (777 mg, 9.13 mmol) and piperidine (542 μL , 466 mg, 5.48 mmol). The crude product was purified by silica-gel column chromatography (gradient: 0-15% MeOH in CH_2Cl_2) to obtain **AFB-6** as a red solid (181 mg, 0.319 mmol, 70%), mp. 210 °C (dec.). ^1H NMR (400 MHz, $\text{DMSO-}d_6$) δ : 7.85 (s, 1H), 7.68-7.56 (m, 6H), 7.51 (dd, $J = 8.6, 2.1$ Hz, 1H), 7.46 (d, $J = 2.2$ Hz, 1H), 7.45-7.40 (m, 2H), 7.32 (t, $J = 7.3$ Hz, 1H), 7.11-7.06 (m, 2H), 3.92 (t, $J = 6.8$ Hz, 2H), 1.75-1.67 (m, 2H), 1.45-1.36 (m, 2H), 1.29-1.22 (m, 4H), 0.85-0.80 (m, 3H) (carboxylic acid proton not visible); ^{13}C NMR (100 MHz, $\text{DMSO-}d_6$) δ : 161.7, 159.9 (dd, $J = 251.6, 8.1$ Hz, 2C), 145.1, 143.2, 143.0, 138.8, 135.5, 134.6, 130.8, 128.9 (2C), 127.1, 126.3, 126.0 (2C), 125.9, 125.2, 125.0, 123.7, 123.4, 121.5, 117.2, 116.1, 115.8, 109.7, 109.1 (d, $J = 25.1$ Hz, 2C), 46.7, 30.8, 26.1, 25.8, 22.1, 13.8; IR (neat, cm^{-1}) ν : 2956 (w), 2925 (w), 2847 (w), 2229 (w), 1627 (m), 1463 (m), 1392 (m), 1197 (m), 1024 (m), 808 (m), 758 (s), 696 (m); HRMS (ASAP+, m/z): 522.1937 (calcd. $\text{C}_{33}\text{H}_{28}\text{N}_2\text{F}_2\text{S}$: 522.1941 [M-CO_2] $^+$); UV (CH_2Cl_2 , 2×10^{-5} M, 22 °C) λ_{max} (nm): 419.5 (10650).

2.5.7 (E)-2-Cyano-3-(2,6-difluoro-4-(10-hexyl-7-(4-methoxyphenyl)-10H-phenothiazin-3-yl)phenyl)acrylate (20)

Compound **15** (410 mg, 0.80 mmol) and ammonium acetate (240 mg, 3.10 mmol) were mixed before acetic acid (4.5 mL) and *tert*-butyl 2-cyanoacetate (0.44 mL, 3.10 mmol) were added under N₂ atmosphere. The reaction mixture was heated to 75 °C and left stirring for 1 hour. Water (30 mL) was added to the solution and the aqueous phase was extracted with EtOAc (3 × 20 mL). The combined organic phases were dried over anhydrous Na₂SO₄, filtered and the solvents were removed in vacuo. Purification by silica-gel column chromatography (*n*-pentane:EtOAc, 14:1, R_f = 0.24) gave compound **20** as a dark red oil (450 mg, 0.69 mmol, 89%). ¹H NMR (400 MHz, DMSO-*d*₆) δ: 8.19 (s, 1H), 7.73-7.68 (m, 4H), 7.58-7.56 (m, 2H), 7.46-7.44 (m, 1H), 7.41-7.40 (m, 1H), 7.09-7.07 (m, 2H), 7.00-6.98 (m, 2H), 3.95-3.90 (m, 2H), 3.78 (s, 3H), 1.75-1.68 (m, 2H), 1.43 (s, 9H), 1.41-1.37 (m, 2H), 1.29-1.24 (m, 4H), 0.85-0.82 (m, 3H); ¹³C NMR (100 MHz, DMSO-*d*₆) δ: 163.3, 159.8 (2C), 158.7, 145.7, 145.3 (d, *J* = 2.0 Hz), 142.42, 142.37, 134.5, 131.2, 130.3, 127.2 (2C), 125.4, 124.5, 123.8, 123.3, 116.4, 115.5 (d, *J* = 55.8 Hz), 114.3 (2C), 111.5, 109.4 (d, *J* = 24.4 Hz, 2C), 84.0, 82.7, 55.1, 46.7, 30.8, 27.5 (3C), 27.4, 26.1, 25.8, 22.0, 13.8 (2 shifts missing); IR (neat, cm⁻¹) ν: 3065 (w), 2925 (w), 2852 (w), 1740 (s), 1719 (s), 1470 (s), 1273 (s), 1242 (s), 1148 (s), 1023 (s), 816 (s); HRMS (ASAP+, *m/z*): 652.2566 (calcd. C₃₉H₃₈F₂N₂O₃S: 652.2571, [M]⁺).

2.5.8 (E)-2-Cyano-3-(2,6-difluoro-4-(10-hexyl-7-(4-methoxyphenyl)-10H-phenothiazin-3-yl)phenyl)acrylic acid (AFB-7)

Compound **20** (300 mg, 0.45 mmol) was stirred in TFA (28 mL) for 1 hour, then the reaction mixture was poured into water (40 mL) and the precipitate that formed was filtered off. The crude product was purified by silica-gel column chromatography (gradient: 0-15% MeOH in CH₂Cl₂) to obtain **AFB-7** as a dark red solid (190 mg, 0.30 mmol, 76%), mp. 115-120 °C (dec.). ¹H NMR (400 MHz, DMSO-*d*₆) δ: 7.86 (s, 1H), 7.65-7.55 (m, 6H), 7.44 (dd, *J* = 8.8, 1.9 Hz, 1H), 7.39 (d, *J* = 2.1 Hz, 1H), 7.05 (d, *J* = 8.6 Hz, 2H), 6.98 (d, *J* = 8.8 Hz, 2H), 3.90 (t, *J* = 6.9 Hz, 2H), 3.78 (s, 3H), 1.73-1.67 (m, 2H), 1.43-1.37 (m, 2H), 1.28-1.22 (m, 4H), 0.85-0.80 (m, 3H) (carboxylic acid proton not visible); ¹³C NMR (100 MHz, DMSO-*d*₆) δ: 162.2,

160.1 (d, $J = 268.3$ Hz, 2C), 158.8, 147.5 (d, $J = 3.1$ Hz), 145.6, 142.5, 140.0, 134.5, 131.2, 130.1, 127.2 (2C), 126.4, 125.4, 125.3, 124.5, 123.8, 123.3, 117.4, 116.2, 116.0 (d, $J = 41.6$ Hz), 115.8, 114.3 (2C), 109.1 (d, $J = 24.9$ Hz, 2C), 98.0, 55.1, 46.6, 30.8, 26.1, 25.8, 22.1, 13.8; IR (neat, cm^{-1}) ν : 2966 (w, br), 2925 (w), 2857 (w), 1703 (m, br), 1631 (s, br), 1465 (s), 1195 (s), 1018 (s), 805 (s); HRMS (ASAP+, m/z): 552.2045 (calcd. $\text{C}_{34}\text{H}_{30}\text{F}_2\text{N}_2\text{OS}$: 552.2047 $[\text{M}-\text{CO}_2]^+$); UV (CH_2Cl_2 , 2×10^{-5} M, 22 °C) λ_{max} (nm): 424.0 (9650).

2.5.9 (*E*)-2-Cyano-3-(5-(10-hexyl-7-phenyl-10H-phenothiazin-3-yl)thiophen-2-yl)acrylic acid (AFB-8)

Dye **AFB-8** was made as described in Section 2.5.1 but starting with compound **16** (222 mg, 0.472 mmol), cyanoacetic acid (803 mg, 9.44 mmol) and piperidine (561 μL , 482 mg, 5.66 mmol). The crude product was purified by silica-gel column chromatography (gradient: 0-15% MeOH in CH_2Cl_2) to obtain **AFB-8** as a dark solid (224 mg, 0.417 mmol, 88%), mp. 209 °C (dec.). ^1H NMR (400 MHz, $\text{DMSO}-d_6$) δ : 8.18 (s, 1H), 7.68 (d, $J = 4.1$ Hz, 1H), 7.63 (d, $J = 7.5$ Hz, 2H), 7.59 (d, $J = 3.8$ Hz, 1H), 7.54-7.49 (m, 3H), 7.46-7.40 (m, 3H), 7.32 (t, $J = 7.3$ Hz, 1H), 7.09 (d, $J = 8.5$ Hz, 1H), 7.06 (d, $J = 8.5$ Hz, 1H), 3.91 (t, $J = 6.9$ Hz, 2H), 1.73-1.67 (m, 2H), 1.43-1.37 (m, 2H), 1.28-1.22 (m, 4H), 0.84-0.80 (m, 3H) (carboxylic acid proton not visible); ^{13}C NMR (100 MHz, $\text{DMSO}-d_6$) δ : 163.6, 148.6, 144.9, 143.2, 141.9, 138.8, 137.5, 135.1, 134.7, 128.9 (2C), 127.2, 127.1, 126.1 (2C), 126.0, 125.5, 125.0, 124.1, 124.0, 123.9, 123.2, 118.6, 116.2, 116.1, 106.6, 46.7, 30.8, 26.1, 25.8, 22.1, 13.8; IR (neat, cm^{-1}) ν : 2956 (w), 2909 (w), 2852 (w), 2213 (w), 1574 (m), 1470 (m), 1389 (s), 1247 (s), 1060 (m), 798 (s), 758 (s), 695 (m); HRMS (ASAP+, m/z): 492.1690 (calcd. $\text{C}_{31}\text{H}_{28}\text{N}_2\text{S}_2$: 492.1694 $[\text{M}-\text{CO}_2]^+$); UV (CH_2Cl_2 , 2×10^{-5} M, 22 °C) λ_{max} (nm): 356.5 (19000), 466.5 (18050).

2.5.10 (E)-2-Cyano-3-(5-(10-hexyl-7-(4-methoxyphenyl)-10H-phenothiazin-3-yl)thiophen-2-yl)acrylic acid (AFB-9)

Dye **AFB-9** was made as described in Section 2.5.1 but starting with compound **17** (189 mg, 0.379 mmol), cyanoacetic acid (644 mg, 7.57 mmol) and piperidine (450 μ L, 387 mg, 4.54 mmol). The crude product was purified by silica-gel column chromatography (gradient: 0-15% MeOH in CH₂Cl₂) to obtain **AFB-9** as a dark solid (165 mg, 0.290 mmol, 77%), mp. 233 °C (dec.); ¹H NMR (400 MHz, DMSO-*d*₆) δ : 8.16 (s, 1H), 7.73 (d, *J* = 3.9 Hz, 1H), 7.58 (d, *J* = 4.1 Hz, 1H), 7.57-7.54 (m, 2H), 7.52-7.49 (m, 2H), 7.44 (dd, *J* = 8.6, 2.1 Hz, 1H), 7.39 (d, *J* = 2.2 Hz, 1H), 7.07-7.03 (m, 2H), 6.98 (d, *J* = 8.6 Hz, 2H), 3.89 (t, *J* = 7.0 Hz, 2H), 3.78 (s, 3H), 1.72-1.66 (m, 2H), 1.42-1.36 (m, 2H), 1.28-1.22 (m, 4H), 0.85-0.80 (m, 3H) (carboxylic acid proton not visible); ¹³C NMR (100 MHz, DMSO-*d*₆) δ : 163.7, 158.7, 148.2, 145.0, 142.5, 141.5, 137.1, 135.1, 134.5, 131.2, 127.2 (2C), 127.0, 125.5, 125.4, 124.5, 124.01, 123.98, 123.8, 123.2, 118.8, 116.2, 116.0, 114.3 (2C), 106.6, 55.2, 46.6, 30.8, 26.1, 25.8, 22.1, 13.8; IR (neat, cm⁻¹) ν : 2950 (w, br), 2924 (w), 2852 (w), 1709 (m), 1688 (m, br), 1579 (s), 1444 (s), 1408 (s), 1236 (s), 1179 (s), 1060 (m), 800 (s); HRMS (ASAP+, *m/z*): 566.1691 (calcd. C₃₃H₃₀N₂O₃S₂: 566.1698 [M]⁺); UV (CH₂Cl₂, 2 \times 10⁻⁵ M, 22 °C) λ_{max} (nm): 360 (16800), 471.0 (15200).

2.5.11 (E)-2-Cyano-3-(5-(10-hexyl-7-phenyl-10H-phenothiazin-3-yl)furan-2-yl)acrylic acid (AFB-10)

Dye **AFB-10** was made as described in Section 2.5.1 but starting with compound **18** (264 mg, 0.583 mmol), cyanoacetic acid (992 mg, 11.7 mmol) and piperidine (693 μ L, 596 mg, 6.99 mmol). The crude product was purified by silica-gel column chromatography (gradient: 0-15% MeOH in CH₂Cl₂) to obtain **AFB-10** as a dark solid (149 mg, 0.285 mmol, 49%), mp. 154 °C (dec.). ¹H NMR (400 MHz, DMSO-*d*₆) δ : 7.89 (s, 1H), 7.72 (dd, *J* = 8.7, 1.9 Hz, 1H), 7.68 (d, *J* = 2.1 Hz, 1H), 7.63 (d, *J* = 7.3 Hz, 2H), 7.51 (dd, *J* = 8.5, 2.1 Hz, 1H), 7.47 (d, *J* = 2.1 Hz, 1H), 7.43 (t, *J* = 7.7 Hz, 2H), 7.35 (d, *J* = 3.5 Hz, 1H), 7.32 (t, *J* = 7.3 Hz, 1H), 7.21 (d, *J* = 3.6 Hz, 1H), 7.14 (d, *J* = 8.7 Hz, 1H), 7.10 (d, *J* = 8.7 Hz, 1H), 3.94 (t, *J* = 6.9 Hz, 2H), 1.74-1.68 (m, 2H), 1.44-1.38 (m, 2H), 1.28-1.22 (m, 4H), 0.85-0.81 (m, 3H) (carboxylic acid proton

not visible); ^{13}C NMR (100 MHz, $\text{DMSO-}d_6$) δ : 160.0, 156.8, 147.7, 145.2, 143.1, 138.7, 135.3, 134.8, 128.9 (2C), 127.2, 126.1 (2C), 126.0, 125.0, 124.4, 123.7, 123.2, 123.1 (2C), 118.0, 116.3, 116.1, 108.5, 102.0, 46.7, 30.8, 26.1, 25.7, 22.1, 13.8 (1 shift is missing); IR (neat, cm^{-1}) ν : 2955 (w), 2917 (w), 2849 (w), 2215 (w), 1686 (w), 1580 (m), 1454 (s), 1390 (m), 1233 (m), 1023 (m), 791 (m), 759 (s), 695 (m); HRMS (ASAP+, m/z): 476.1922 (calcd. $\text{C}_{31}\text{H}_{28}\text{N}_2\text{OS}$: 476.1922 [M-CO_2] $^+$); UV (CH_2Cl_2 , 2×10^{-5} M, 22 $^\circ\text{C}$) λ_{max} (nm): 363.0 (14850), 479.5 (19150).

2.5.12 (E)-2-Cyano-3-(5-(10-hexyl-7-(4-methoxyphenyl)-10H-phenothiazin-3-yl)furan-2-yl)acrylate (21)

Compound **21** was made as described in Section 2.5.7 but starting with compound **19** (170 mg, 0.40 mmol), ammonium acetate (110 mg, 1.40 mmol), *tert*-butyl 2-cyanoacetate (0.20 mL, 1.40 mmol) in acetic acid (2.0 mL). The crude product was purified by silica-gel column chromatography (*n*-pentane: EtOAc, 19:1, $R_f = 0.49$) gave compound **21** as a dark red oil (120 mg, 0.198 mmol, 55%). ^1H NMR (400 MHz, $\text{DMSO-}d_6$) δ : 7.99 (s, 1H), 7.75-7.74 (m, 1H), 7.71-7.70 (m, 1H), 7.59-7.57 (m, 2H), 7.56-7.55 (m, 1H), 7.47-7.45 (m, 1H), 7.42-7.41 (m, 1H), 7.31-7.30 (m, 1H), 7.17-7.15 (m, 1H), 7.10-7.09 (m, 1H), 7.00-6.98 (m, 2H), 3.96-3.90 (m, 2H), 3.78 (s, 3H), 1.74-1.69 (m, 2H), 1.43 (s, 9H), 1.43-1.41 (m, 2H), 1.27-1.25 (m, 4H), 0.85-0.82 (m, 3H); ^{13}C NMR (100 MHz, $\text{DMSO-}d_6$) δ : 163.3, 158.6, 158.5, 147.1, 144.8, 143.2, 137.2, 134.0, 130.7, 127.4 (2C), 127.2, 125.1, 124.8, 124.6, 123.2, 123.0, 122.62, 122.61, 116.43, 116.42, 116.1, 114.7 (2C), 109.4, 95.0, 83.6, 55.1, 46.6, 30.8, 27.6 (3C), 26.1, 25.7, 22.0, 13.8; IR (neat, cm^{-1}) ν : 3138 (w), 2977 (w), 2930 (w), 2870 (w), 2262 (w), 2218 (w), 1740 (s), 1714 (s), 1610 (s), 1583 (s), 1456 (s), 1236 (s), 1152 (s), 1028 (s), 798 (s), 587 (m); HRMS (ASAP+, m/z): 606.2548 (calcd. $\text{C}_{37}\text{H}_{38}\text{N}_2\text{O}_4\text{S}$: 606.2552, [M] $^+$).

2.5.13 (E)-2-Cyano-3-(5-(10-hexyl-7-(4-methoxyphenyl)-10H-phenothiazin-3-yl)furan-2-yl)acrylic acid (AFB-11)

Dye **AFB-11** was made as described in Section 2.5.8 but starting with compound **21** (120 mg, 0.19 mmol) in TFA (12 mL). The crude product was purified by silica-gel column chromatography (gradient: 0-15% MeOH in CH₂Cl₂) to obtain **AFB-11** as a black solid (83 mg, 0.15 mmol, 79%), mp. 155-160 °C (dec.). ¹H NMR (400 MHz, DMSO-*d*₆) δ: 7.83 (s, 1H), 7.70 (dd, *J* = 8.5, 2.2 Hz, 1H), 7.66 (d, *J* = 2.1 Hz, 1H), 7.57 (d, *J* = 8.8 Hz, 2H), 7.45 (dd, *J* = 8.4, 2.1 Hz, 1H), 7.41 (d, *J* = 2.1 Hz, 1H), 7.27 (d, *J* = 3.6 Hz, 1H), 7.18 (d, *J* = 3.6 Hz, 1H), 7.12 (d, *J* = 8.8 Hz, 1H), 7.07 (d, *J* = 8.6 Hz, 1H), 6.98 (d, *J* = 8.8 Hz, 2H), 3.92 (t, *J* = 6.9 Hz, 2H), 3.78 (s, 3H), 1.75-1.66 (m, 2H), 1.45-1.36 (m, 2H), 1.29-1.21 (m, 4H), 0.85-0.80 (m, 3H) (carboxylic acid proton not visible); ¹³C NMR (100 MHz, DMSO-*d*₆) δ: 164.0, 158.7, 156.1, 147.9, 145.1, 142.5, 134.6, 131.2, 127.2 (2C), 125.5, 125.4, 124.5, 124.2, 123.7, 123.3, 123.1, 122.9, 118.7, 116.3, 116.0, 114.3 (2C), 113.6, 108.2, 95.4, 55.2, 46.7, 30.8, 26.1, 25.7, 22.1, 13.8; IR (neat, cm⁻¹) ν: 3132 (w, br), 2956 (w), 2919 (w), 2847 (w), 2213 (w), 1683 (s, br), 1579 (s), 1455 (s), 1418 (s), 1236 (s), 1034 (s), 935 (w), 790 (s); HRMS (ASAP+, *m/z*): 506.2024 (calcd. C₃₂H₃₀N₂O₄S: 506.2028 [M-CO₂]⁺); UV (CH₂Cl₂, 2 × 10⁻⁵ M, 22 °C): λ_{max} (nm): 362.5 (14200), 473.0 (14800).

3 Results and Discussion

To investigate the realm of π -spacers for phenothiazine dyes, we planned for the synthesis of 10 new dyes having five different π -spacers. In terms of π -spacers, thiophenes are the common choice, although dyes containing furans are not uncommon. [28, 29] We also incorporated phenyl, *meta*-fluorophenyl and 3,5-difluorophenyl to investigate six-membered spacers and electron withdrawing fluorine substituents. All these variants were made using two different auxiliary donors (*para*-methoxyphenyl and phenyl). Additionally, as a reference dye **AFB-1** was prepared without a π -spacer. To prevent aggregation a hexyl chain was installed at the phenothiazine core, as this chain length previously has been found efficient for phenothiazine sensitizers. [30]

3.1 Synthesis

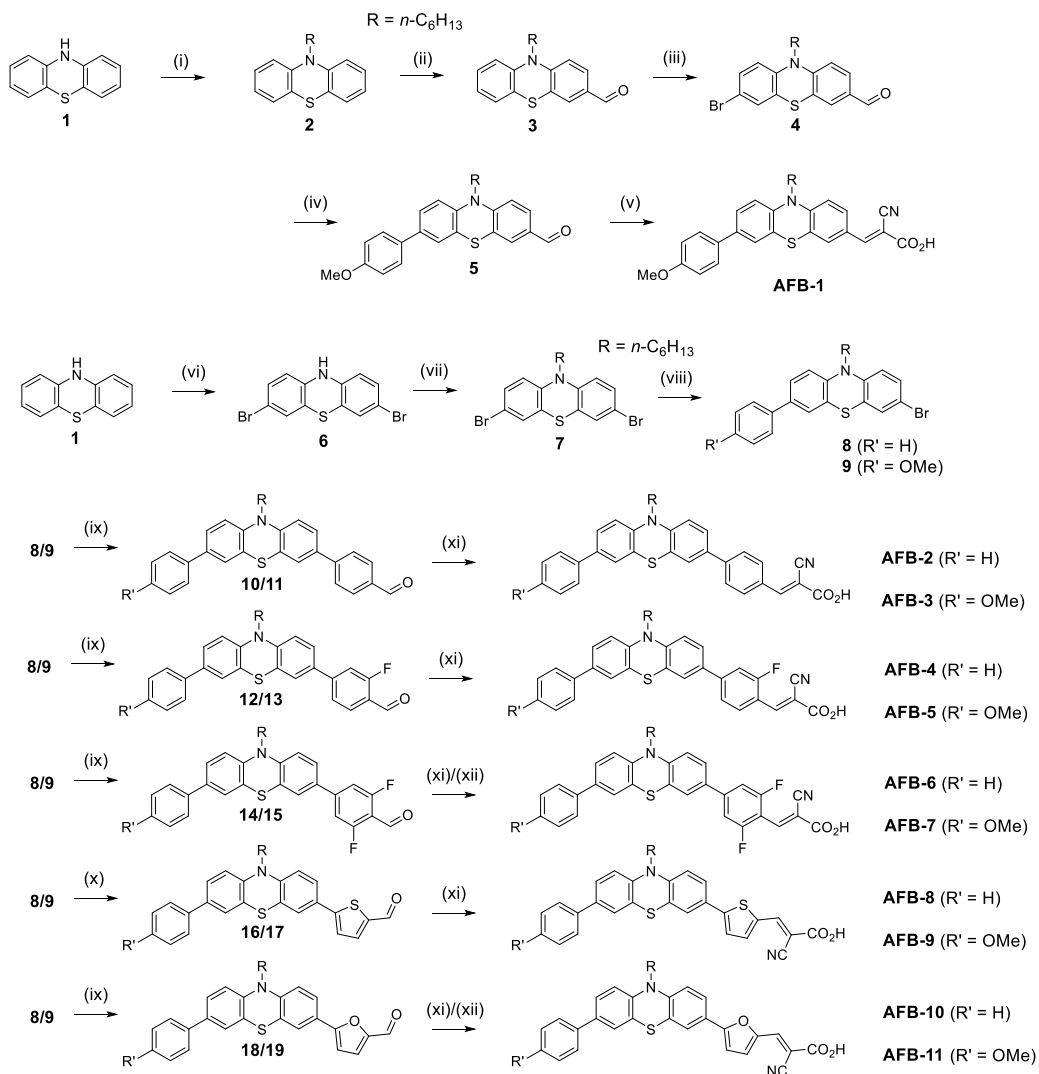
Dye **AFB-1** without π -spacer was synthesized by *N*-alkylation of 10*H*-phenothiazine, followed by a Vilsmeier-Haack formylation and a subsequent bromination by NBS. Then, a Suzuki coupling introduced the 4-methoxyphenyl auxiliary donor before the Knoevenagel condensation assembled the cyanoacrylic acid anchoring group, as shown in Scheme 1.

To synthesize the other dyes the key building block 3,7-dibromo-10-hexyl-10*H*-phenothiazine (**7**) was needed. It was synthesized in two steps from 10*H*-phenothiazine by bromination in acetic acid followed by *N*-alkylation with 1-bromohexane as shown in Scheme 1. [31, 32] Further, the different auxiliary donors were introduced by Suzuki cross-couplings with either 4-methoxyphenylboronic acid or phenylboronic acid, yielding the unsymmetrical building blocks **8** and **9**. This reaction displayed very low chemoselectivity, and a near statistical distribution of products was obtained. To maximize the amount of the desired coupling products **8** and **9**, only 1.1 equivalents of arylboronic acid was used, resulting in a 1:2:1 distribution of starting material, monocoupled and dicoupled product. Purification by silica-gel column chromatography was facile, also allowing for recovery of building block **7**.

The dyes with furan (**AFB-10** and **AFB-11**), phenyl (**AFB-2** and **AFB-3**), *meta*-fluorophenyl (**AFB-4** and **AFB-5**) and 3,5-difluorophenyl (**AFB-6** and **AFB-7**) as π -spacers were prepared in a subsequent Suzuki

coupling of the building blocks **8** and **9**. This was followed by a Knoevenagel condensation with cyanoacetic acid as described by Iqbal et al. [33] However, finding a reliable procedure for coupling the building blocks **8** or **9** with 5-formyl-2-thienylboronic acid proved difficult, as these reactions were usually plagued by low conversion.

Instead, the building blocks **8** and **9** were first converted to their pinacol boronic esters in a palladium catalyzed coupling with $\text{PdCl}_2(\text{CH}_3\text{CN})_2$, SPhos and pinacol borane by the protocol developed by Billingsley and Buchwald. [34] Without further purification, these were then coupled with 5-bromo-2-thiophenecarboxaldehyde using $\text{Pd}(\text{OAc})_2$, SPhos and K_2CO_3 in 1,4-dioxane and water. This gave the aldehydes **16** and **17** which were further converted in Knoevenagel condensations to **AFB-8** (R = H) and **AFB-9** (R = OMe). The dyes **AFB-7** and **AFB-11** were prepared via their *tert*-butyl cyanoacrylate analogs, with subsequent TFA hydrolysis to yield the final dyes. This was a more tedious route using harsher chemicals and two steps rather than one. As a result, this approach was abandoned in our further studies.



Scheme 1. Synthesis of dyes **AFB-1** to **AFB-11**. i) NaH, 1-bromohexane, ii) DMF, POCl₃, iii) NBS, iv) Pd(PPh₃)₄, 4-methoxyphenylboronic acid, K₂CO₃, v) cyanoacetic acid, piperidine, vi) Br₂, vii) NaH, 1-bromohexane, viii) Pd(PPh₃)₄, phenylboronic acid/4-methoxyphenylboronic acid, K₂CO₃, ix) Pd(OAc)₂, SPhos, arylboronic acid, K₂CO₃, x) PdCl₂(CH₃CN)₂, Et₃N, pinacol borane, then Pd(OAc)₂, SPhos, K₂CO₃, 5-bromo-2-thiophenecarboxaldehyde xi) cyanoacetic acid, piperidine, xii) tert-butyl 2-cyanoacetate, ammonium acetate, then TFA hydrolysis.

3.2 Photophysical properties

UV-Visible absorption spectrum of all dyes in solution (2×10^{-5} M in CH_2Cl_2 , Figure 2) and on TiO_2 (Figure S3) shows a clear distinction between the five- and six-membered π -spacers, where the former dyes were considerably redshifted and had higher extinction coefficients than the latter. In order to obtain the values for the optical bandgaps, the emission spectra were normalized with respect to the internal charge transfer (ICT) transition peaks in the absorption spectra, and the intersect of these curves gives the bandgap energy. [35] All the photophysical properties are summarized in Table 1. Interestingly, **AFB-1** without any π -spacer showed similar λ_{max} to the dyes with five-membered spacers, albeit with a slightly lower extinction coefficient. These observations could indicate that a phenyl-based π -spacer is too large, twisting the aromatic system causing a weaker ICT process from the donor to the acceptor moieties, thus favoring the smaller five-membered π -spacers, and even no π -spacer.

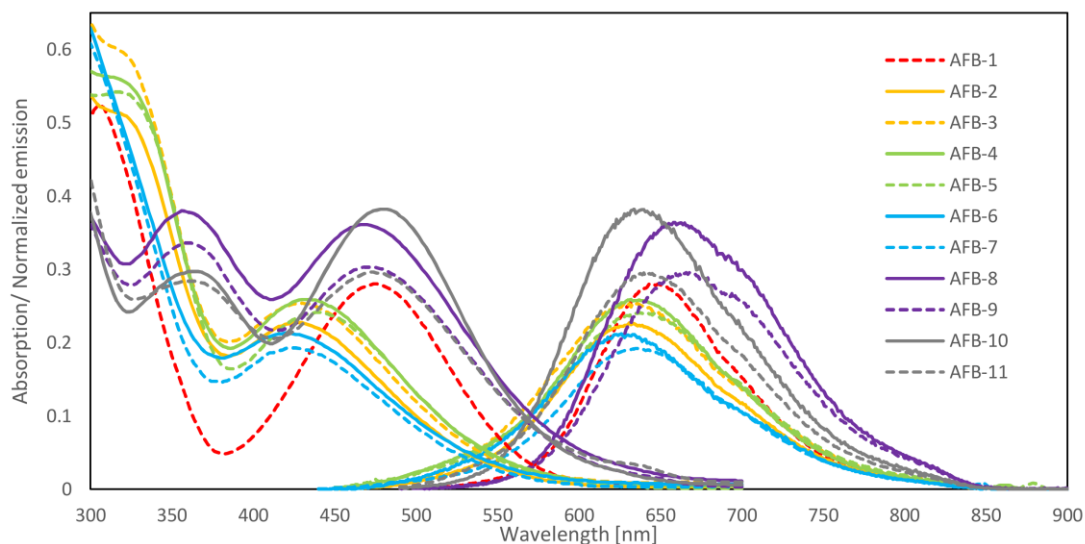



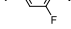

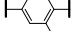
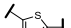
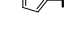
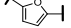



Figure 2. Absorption spectra and normalized emission spectra for all dyes. The intersection of the absorption and normalized emission spectra gives $E_{g_{\text{opt}}}$. Each dye is excited at its ICT transition maximum absorption wavelength.

Table 1. Photophysical properties from spectroscopy and electrochemical measurements. The absorption spectra were measured in CH_2Cl_2 , emission in $CHCl_3$.

Dye	Donor R gr.	π - linker	Absorption [nm]			Emmision λ_{max} [nm]	E_{HOMO} vs. NHE [V]	E_{LUMO} vs. NHE [V]	$E_{g_{chem}}$ [V]	$E_{g_{opt}}$ [eV] ^a
			λ_{max} ,	ϵ [$M^{-1}cm^{-1}$]	λ_{max} ,					
			sol		TiO ₂					
AFB-1	OMe	None	475.0	14000	411.5	649	0.88	-1.30 ^c	n/a	2.18
AFB-2	H		425.0	11350	n/a ^b	631	0.75	-1.57	2.32	2.33
AFB-3	OMe		429.0	12700	n/a ^b	633	0.80	-1.40	2.20	2.33
AFB-4	H		431.5	12950	n/a ^b	632	0.73	-1.58	2.31	2.33
AFB-5	OMe		440.5	12050	n/a ^b	641	0.68	-1.66	2.34	2.34
AFB-6	H		419.5	10650	n/a ^b	626	0.76	-1.61 ^c	n/a	2.37
AFB-7	OMe		424.0	9650	n/a ^b	635	0.74	-1.64 ^c	n/a	2.38
AFB-8	H		466.5	18050	412.5	658	0.75	-1.35	2.10	2.12
AFB-9	OMe		471.0	15200	411.0	659	0.81	-1.31 ^c	n/a	2.12
AFB-10	H		479.5	19150	415.0	634	0.75	-1.50	2.25	2.18
AFB-11	OMe		473.0	14800	408.0	640	0.67	-1.61	2.28	2.19

^a $E_{g_{opt}}$ was calculated from the intersection of the absorption and normalized emission spectra.

^b No clear peak to assign.

^c Calculated from the optical band gap ($E_{HOMO} - E_{g_{opt}}$).

Adsorption of the dyes onto TiO₂ films resulted in blueshifts of the absorption maxima in the range of 50-60 nm (Supplementary information, Fig. S3). Deprotonation of the dye molecules in solution using triethylamine also led to blueshifts (Fig. S2), but not of the same magnitude as when adsorbed onto TiO₂. Figure 3 compares the absorption of the four dyes with five-membered π -spacers in solution, deprotonated in solution and on TiO₂. This suggests there is an additional effect leading to further blueshifting of the absorption in addition to deprotonation, which is likely to be due to H-aggregation. [13] The deprotonated absorption spectra are generally in good accordance with the spectra from the TiO₂ films, suggesting deprotonation of the dye molecules could be an easy way of simulating the UV/Vis-properties when adsorbed on the TiO₂ photocathode.

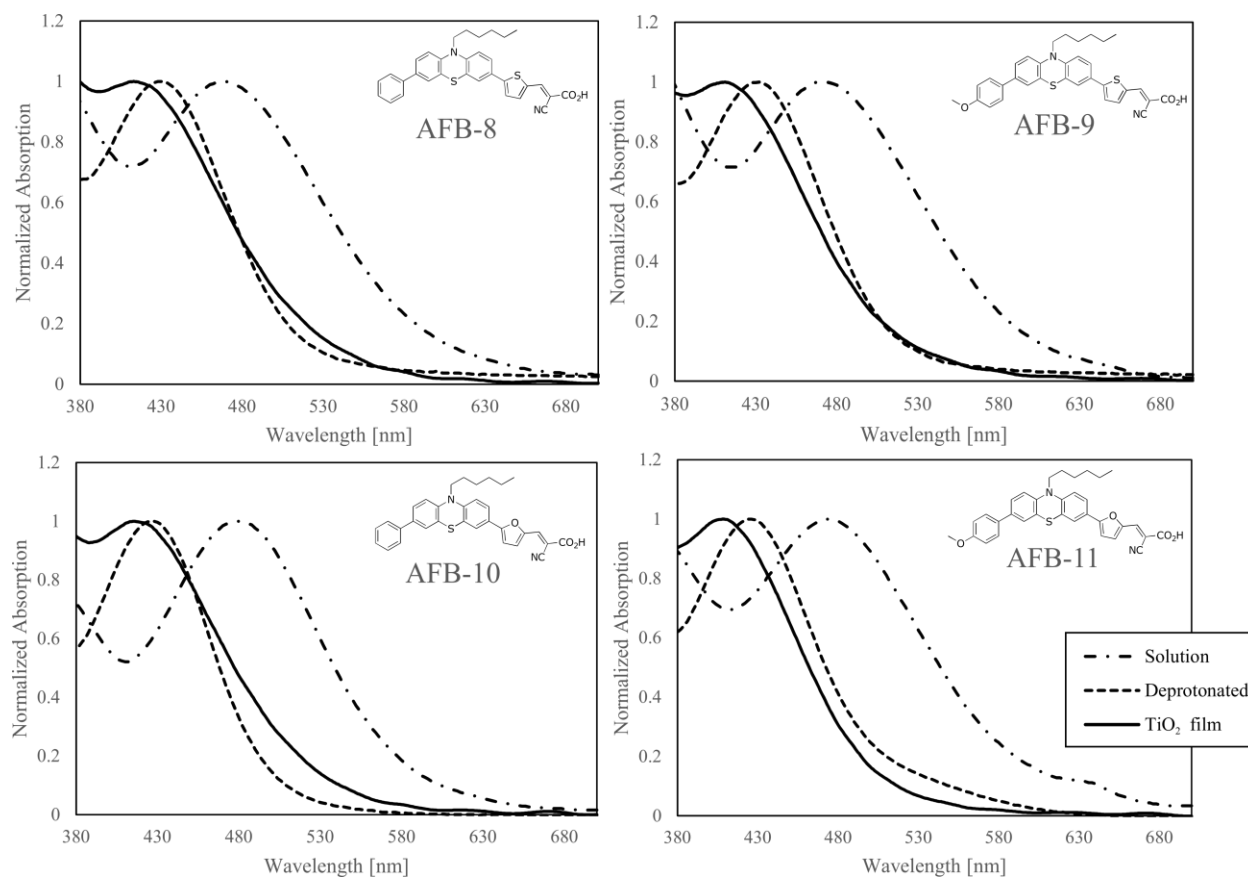


Figure 3. Absorption spectra of **AFB-8**, **AFB-9**, **AFB-10** and **AFB-11** in solution, deprotonated in solution and on TiO_2 films. The staining solution concentration was 0.5 mM in THF:acetonitrile (57:43, v:v) with 5 mM of CDCA. Deprotonation in solution was done with a drop of triethylamine into the UV cuvette.

3.3 Electrochemical properties

The energy levels of **AFB-1** to **AFB-11** were probed using electrochemistry to determine their position relative to the energy levels of the conduction band of TiO_2 and the redox shuttle I^-/I_3^- . Due to poor film forming properties, solution electrochemistry was employed. Cyclic voltammetry in solution for the “parent” phenothiazine building block **7** shows a very characteristic spectrum with one fully reversible process at $E_{1/2} = 0.43$ V vs Fc/Fc^+ and 3 quasi reversible processes at 1.01, 1.10 and 1.29 V. (Fig. S5) The first process is attributed to the one electron process of the phenothiazine core and the formation of the radical cation. This characteristic electrochemical process is in good agreement with other phenothiazine-based molecules reported in the literature. [36, 37] The processes observed at higher voltages are most

likely the result of excimers or aggregates forming close to the electrode surface, similar to previous reports with related phenothiazine-containing molecules. [38, 39] However, this will require additional electrochemical experimentation and lies beyond the scope of this manuscript. Differential pulse voltammetry (DPV) was also employed to provide additional electrochemical information due to its virtue of removing the effect of electrode capacitive charging. This results in only faradaic processes and thus much higher signals than other conventional voltammetry methods can be achieved. [40]

All the energy levels are reported vs. NHE in Table 1 and corresponding DPV spectra of all the dyes are shown in Supporting information (Fig. S7). The ionization potentials (HOMO level) for all the dyes were found to be between 0.67 and 0.88 V with **AFB-1** having the deepest ionization potential. In general, the electrochemical data show small differences of ± 0.1 V with regards to the HOMO levels of the dyes with different auxiliary donors. Exchanging the π -spacer, on the other hand, affects primarily the LUMO level of the dye, allowing for a ± 0.3 V tuning of this energy level. For the instances where the LUMO levels were extracted from the DPV measurements, the band gaps were in agreement with optical bandgaps. The electrochemical measurements confirm that the HOMO energy levels of the sensitizers are well below what is required for the dyes to be regenerated by the I/I_3^- electrolyte and the corresponding bandgaps ensure the LUMO levels are well above the conduction band edge of TiO_2 to ensure efficient electron injection, as illustrated for the 4-methoxyphenyl series of dyes in Figure 4.

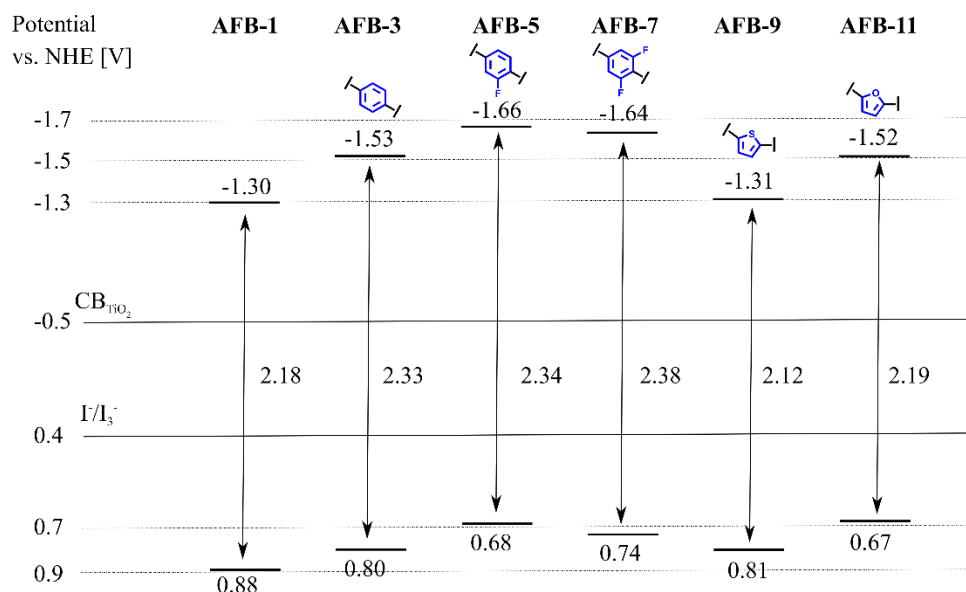


Figure 4. HOMO and LUMO levels for the series of dyes with the 4-methoxyphenyl auxiliary donor. HOMO levels determined from DPV electrochemical measurements, and LUMO levels are derived from the optical band gaps.

3.4 Photovoltaic performance

DSSC devices were fabricated from all 11 sensitizers, in order to investigate their current-voltage characteristics. Figure 5 shows the I-V curves of the best cells from three parallels, while average values with standard deviation are given in Table 2. The photovoltaic performance of the five-membered π -spacer dyes was better than the dyes with phenyl-based spacers, as would be expected from the differences found in the UV/Vis measurements. In particular, the photocurrent from these cells was higher, resulting in elevated PCE values. The fill factors and open-circuit voltages were mostly unaffected by the nature of the π -spacer. This shows that the differences between the five- and six-membered π -spacers are equally apparent in devices as seen from their absorption behavior in solution.

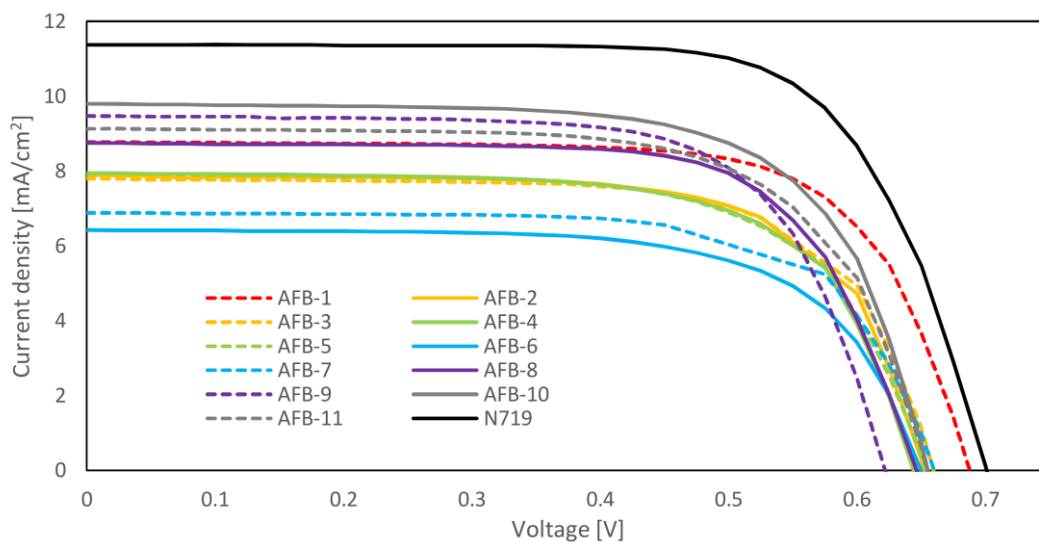
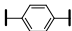
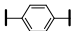
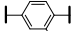
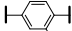
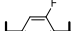
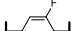
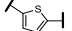
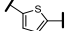
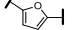
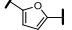


Figure 5. I-V curves for all dyes under 1 sun AM1.5G illumination. The curve from the best cell from each parallel is included.

Table 2. Photovoltaic properties from DSSC's fabricated with all 11 dyes. All values are averages from three cells. Standard deviation for all parameters can be found in Table S2.

Dye ^a	Donor R	π -linker	J _{sc}	V _{oc}	FF	PCE [%]	IPCE [%]	IPCE J _{sc}
	gr.		[mA/cm ²]	[V]			at λ_{\max}	[mA/cm ²] ^c
AFB-1	OMe	None	8.64	0.68	0.71	4.15 ± 0.17	77 (510)	9.20
AFB-2	H		7.83	0.66	0.68	3.53 ± 0.04	75 (500)	8.16
AFB-3	OMe		7.83	0.66	0.67	3.46 ± 0.14	75 (500)	8.56
AFB-4	H		7.63	0.65	0.69	3.43 ± 0.07	71 (510)	8.74
AFB-5	OMe		7.87	0.65	0.67	3.41 ± 0.05	69 (510)	9.03
AFB-6	H		6.28	0.65	0.68	2.79 ± 0.02	67 (490)	7.27
AFB-7	OMe		6.77	0.66	0.67	2.96 ± 0.06	67 (490)	7.57
AFB-8	H		9.14	0.63	0.68	3.87 ± 0.08	71 (510)	9.68
AFB-9	OMe		9.56	0.62	0.68	4.03 ± 0.03	73 (510)	10.48
AFB-10	H		9.44	0.67	0.69	4.34 ± 0.05	77 (510)	10.44
AFB-11	OMe		9.15	0.65	0.67	3.97 ± 0.05	74 (510)	9.88
N719^b		-	11.32	0.69	0.72	5.64 ± 0.04	75 (540)	12.44

^a Thickness of active TiO₂ was 12.5 μ m and scattering layer was 5 μ m. Electrolyte contained 0.5 M 1-butyl-3-methylimidazolium iodide, 0.1 M lithium iodide, 0.05 M I₂ and 0.5 M *tert*-butylpyridine in acetonitrile.

^b Staining solution for N719 (from Solaronix) was ethanol.

^c IPCE spectra integrated and normalized according to the ASTM G173 AM 1.5 G solar spectrum available from NREL (<http://rredc.nrel.gov/solar/spectra/am1.5/>).

The thiophene π -spacer is a very popular moiety in metal-free sensitizers for DSSCs, and these dyes were expected to perform well in this study. Furan is less commonly used, but has outperformed thiophene as a π -spacer in some previous studies [21, 22]. This can be attributed to the smaller ring size of furan compared to thiophene, which result in a lower dihedral angle and better orbital overlap between phenothiazine and the π -spacer plane.

Another surprising finding was the poor performance of the 3,5-difluorophenyl containing dyes (**AFB-6** and **AFB-7**). This π -spacer has previously been reported to enhance the efficiency compared to a plain phenyl ring [20, 41], while quite the opposite was observed in this study.

Alkoxy substituted phenyls are common auxiliary donors, providing extra electron donation and the long alkyl chains prevent aggregation. The methoxy group should be able to provide the additional electron donation without affecting aggregation. However, no clear effect from the methoxy substitution could be extracted from the dyes in this study.

The IPCE spectra were recorded for the best performing cell in each parallel of three, and the curves are plotted in Figure 6, while the peak values and corresponding integrated short circuit current are given in Table 2. The calculated J_{sc} values from the IPCE spectra are 0.33-1.16 mA/cm² higher compared to those obtained under one sun illumination. This small difference could be due to different light intensities and the spectral mismatch from the Xenon solar simulator lamp.

The IPCE curves of the dyes with thiophene and furan π -spacers show the widest action spectra, compared to the narrower peaks of the six-membered dyes. The difluoro containing dyes **AFB-6** and **AFB-7** have the lowest and narrowest IPCE spectra of the series, while the furan based **AFB-10** has the highest plateau of all the dyes.

Although the efficiency of the reference dye **AFB-1** is the second highest in the series, its IPCE spectrum is significantly narrower compared to the dyes with five-membered π -spacers. Further efforts should be focused on increasing the absorption of the sensitizers. From this study, it is clear that in order to improve the impact of π -spacers for the phenothiazine scaffold, it is necessary to extend the conjugation further than thiophene or furan. Meanwhile, not distorting the orbital overlap between the phenothiazine core and the anchoring group is of high importance, and other challenges related to aggregation from π - π stacking may occur when increasing the size of the π -spacers.

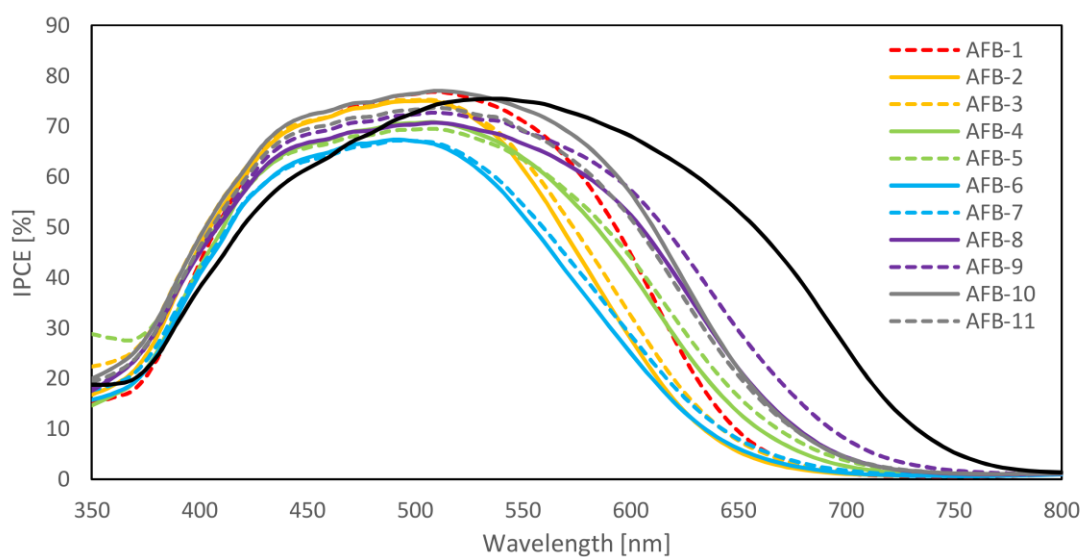


Figure 6. IPCE spectra of all dyes.

4 Conclusion

We have delved into the realm of π -spacers for phenothiazine sensitizers in DSSCs, and eleven new dyes have been synthesized. The aim of this study was to compare the impact of five different π -spacers in two complementary series of dyes, including a dye with no π -spacer. The five membered π -spacers thiophene and furan were found to be superior to the six membered π -spacer dyes, with furan performing marginally better than thiophene. To our surprise, the general effect of introducing a π -spacer was not always positive, as demonstrated by the reference dye **AFB-1**, which outperformed all but the best furan dye, **AFB-10**.

To further improve this class of sensitizers, the use of π -spacers based on five membered heterocycles is a viable solution, but the conjugation should be increased beyond one thiophene or furan unit. Naturally, increasing the electron donating power of the phenothiazine donor could also improve the efficiency further, which can be achieved by altering and increasing the number of auxiliary donors.

Acknowledgements

The authors would like to thank the NV-faculty and the Department of Chemistry at NTNU for financial support, engineer Julie Asmussen and Dr. Susana Villa Gonzalez for HRMS analyses, Roger Aarvik for technical support and MSc Henrik Holthe Kringhaug for the synthesis of the precursors of **AFB-1**. The Research Council of Norway is acknowledged for the support to the Norwegian Micro- and Nano-Fabrication Facility, NorFab, project number 245963/F50.

References

- [1] O'Regan B., Grätzel M. A low-cost, high-efficiency solar cell based on dye-sensitized colloidal TiO₂ films. *Nature*. 1991;353:737-740.
- [2] Freitag M., Teuscher J., Saygili Y., Zhang X., Giordano F., Liska P., et al. Dye-sensitized solar cells for efficient power generation under ambient lighting. *Nat. Photonics*. 2017;11:372-378.
- [3] Jacoby M. The future of low-cost solar cells *Chem. Eng. News*. 2016;94:30-35.
- [4] Freitag M., Daniel Q., Pazoki M., Sveinbjörnsson K., Zhang J., Sun L., et al. High-efficiency dye-sensitized solar cells with molecular copper phenanthroline as solid hole conductor. *Energy Environ. Sci*. 2015;8:2634-2637.
- [5] Freitag M., Giordano F., Yang W., Pazoki M., Hao Y., Zietz B., et al. Copper Phenanthroline as a Fast and High-Performance Redox Mediator for Dye-Sensitized Solar Cells. *J. Phys. Chem. C*. 2016;120:9595-9603.
- [6] Hao Y., Yang W., Zhang L., Jiang R., Mijangos E., Hammarström L., et al. A small electron donor in cobalt complex electrolyte significantly improves efficiency in dye-sensitized solar cells. *Nat. Commun*. 2016;7:13934.
- [7] Yum J.-H., Baranoff E., Kessler F., Moehl T., Ahmad S., Bessho T., et al. A cobalt complex redox shuttle for dye-sensitized solar cells with high open-circuit potentials. *Nat. Commun*. 2012;3:631.

- [8] Kakiage K., Aoyama Y., Yano T., Oya K., Fujisawa J.-i., Hanaya M. Highly-efficient dye-sensitized solar cells with collaborative sensitization by silyl-anchor and carboxy-anchor dyes. *Chem. Commun.* 2015;51:15894-15897.
- [9] Robertson N. Optimizing dyes for dye-sensitized solar cells. *Angew. Chem. Int. Ed.* 2006;45:2338-2345.
- [10] Higashino T., Imahori H. Porphyrins as excellent dyes for dye-sensitized solar cells: recent developments and insights. *Dalton Trans.* 2015;44:448-463.
- [11] Mathew S., Yella A., Gao P., Humphry-Baker R., Curchod B. F. E., Ashari-Astani N., et al. Dye-sensitized solar cells with 13% efficiency achieved through the molecular engineering of porphyrin sensitizers. *Nat. Chem.* 2014;6:242-247.
- [12] Ahmad S., Guillen E., Kavan L., Grätzel M., Nazeeruddin M. K. Metal free sensitizer and catalyst for dye sensitized solar cells. *Energy Environ. Sci.* 2013;6:3439-3466.
- [13] Mishra A., Fischer M. K., Bäuerle P. Metal-free organic dyes for dye-sensitized solar cells: from structure: property relationships to design rules. *Angew. Chem. Int. Ed.* 2009;48:2474-2499.
- [14] Sheibani E., Zhang L., Liu P., Xu B., Mijangos E., Boschloo G., et al. A study of oligothiophene-acceptor dyes in p-type dye-sensitized solar cells. *RSC Adv.* 2016;6:18165-18177.
- [15] Tian H., Yang X., Chen R., Pan Y., Li L., Hagfeldt A., et al. Phenothiazine derivatives for efficient organic dye-sensitized solar cells. *Chem. Commun.* 2007:3741-3743.
- [16] Tian H., Yang X., Cong J., Chen R., Liu J., Hao Y., et al. Tuning of phenoxazine chromophores for efficient organic dye-sensitized solar cells. *Chem. Commun.* 2009:6288-6290.
- [17] Lin R. Y.-Y., Wu F.-L., Li C.-T., Chen P.-Y., Ho K.-C., Lin J. T. High-Performance Aqueous/Organic Dye-Sensitized Solar Cells Based on Sensitizers Containing Triethylene Oxide Methyl Ether. *ChemSusChem.* 2015;8:2503-2513.
- [18] Luo J.-S., Wan Z.-Q., Jia C.-Y. Recent advances in phenothiazine-based dyes for dye-sensitized solar cells. *Chin. Chem. Lett.* 2016;27:1304-1318.

- [19] Huang Z.-S., Meier H., Cao D. Phenothiazine-based dyes for efficient dye-sensitized solar cells. *J. Mater. Chem. C*. 2016;4:2404-2426.
- [20] Lee M.-W., Kim J.-Y., Son H. J., Kim J. Y., Kim B., Kim H., et al. Tailoring of Energy Levels in D- π -A Organic Dyes via Fluorination of Acceptor Units for Efficient Dye-Sensitized Solar Cells. *Sci. Rep.* 2015;5:7711.
- [21] Wan Z., Jia C., Duan Y., Zhou L., Lin Y., Shi Y. Phenothiazine-triphenylamine based organic dyes containing various conjugated linkers for efficient dye-sensitized solar cells. *J. Mater. Chem.* 2012;22:25140-25147.
- [22] Kim S. H., Kim H. W., Sakong C., Namgoong J., Park S. W., Ko M. J., et al. Effect of Five-Membered Heteroaromatic Linkers to the Performance of Phenothiazine-Based Dye-Sensitized Solar Cells. *Org. Lett.* 2011;13:5784-5787.
- [23] Bhim Raju T., Vaghasiya J. V., Afroz M. A., Soni S. S., Iyer P. K. Design, synthesis and DSSC performance of o-fluorine substituted phenylene spacer sensitizers: effect of TiO₂ thickness variation. *Phys. Chem. Chem. Phys.* 2016;18:28485-28491.
- [24] Bodedla G. B., Thomas K. R. J., Li C.-T., Ho K.-C. Functional tuning of phenothiazine-based dyes by a benzimidazole auxiliary chromophore: an account of optical and photovoltaic studies. *RSC Adv.* 2014;4:53588-53601.
- [25] Hao Y., Gabrielsson E., Lohse P. W., Yang W., Johansson E. M. J., Hagfeldt A., et al. Peripheral Hole Acceptor Moieties on an Organic Dye Improve Dye-Sensitized Solar Cell Performance. *Adv. Sci.* 2015;2:1500174.
- [26] Ozawa H., Awa M., Ono T., Arakawa H. Effects of Dye-Adsorption Solvent on the Performances of the Dye-Sensitized Solar Cells Based on Black Dye. *Chem. Asian. J.* 2012;7:156-162.
- [27] Joly D., Pellejà L., Narbey S., Oswald F., Chiron J., Clifford J. N., et al. A Robust Organic Dye for Dye Sensitized Solar Cells Based on Iodine/Iodide Electrolytes Combining High Efficiency and Outstanding Stability. *Sci. Rep.* 2014;4:4033.

- [28] Hao Y., Saygili Y., Cong J., Eriksson A., Yang W., Zhang J., et al. Novel Blue Organic Dye for Dye-Sensitized Solar Cells Achieving High Efficiency in Cobalt-Based Electrolytes and by Co-Sensitization. *ACS Appl. Mater. Interfaces*. 2016;8:32797-32804.
- [29] Liu P., Sharmoukh W., Xu B., Li Y. Y., Boschloo G., Sun L., et al. Novel and Stable D–A– π –A Dyes for Efficient Solid-State Dye-Sensitized Solar Cells. *ACS Omega*. 2017;2:1812-1819.
- [30] Hua Y., Chang S., Huang D. D., Zhou X., Zhu X. J., Zhao J. Z., et al. Significant Improvement of Dye-Sensitized Solar Cell Performance Using Simple Phenothiazine-Based Dyes. *Chem. Mater*. 2013;25:2146-2153.
- [31] Elkassih S. A., Sista P., Magurudeniya H. D., Papadimitratos A., Zakhidov A. A., Biewer M. C., et al. Phenothiazine Semiconducting Polymer for Light-Emitting Diodes. *Macromol. Chem. Phys*. 2013;214:572-577.
- [32] Hurt C. R., Lingappa V., Freeman B., Atuegbu A., Kitaygorodskyy A. Phenothiazine derivatives as antiviral agents and their preparation, pharmaceutical compositions and use in the treatment of viral infections. 2014. Patent US 8759336B2.
- [33] Iqbal Z., Wu W.-Q., Huang Z.-S., Wang L., Kuang D.-B., Meier H., et al. Trilateral π -conjugation extensions of phenothiazine-based dyes enhance the photovoltaic performance of the dye-sensitized solar cells. *Dyes Pigments*. 2016;124:63-71.
- [34] Billingsley K. L., Buchwald S. L. An Improved System for the Palladium-Catalyzed Borylation of Aryl Halides with Pinacol Borane. *J. Org. Chem*. 2008;73:5589-5591.
- [35] Pazoki M., Cappel U. B., Johansson E. M. J., Hagfeldt A., Boschloo G. Characterization techniques for dye-sensitized solar cells. *Energy & Environmental Science*. 2017;10:672-709.
- [36] Nagarajan B., Kushwaha S., Elumalai R., Mandal S., Ramanujam K., Raghavachari D. Novel ethynyl-pyrene substituted phenothiazine based metal free organic dyes in DSSC with 12% conversion efficiency. *J. Mater. Chem. A*. 2017;5:10289-10300.

- [37] Xie Z., Midya A., Loh K. P., Adams S., Blackwood D. J., Wang J., et al. Highly efficient dye-sensitized solar cells using phenothiazine derivative organic dyes. *Prog. Photovolt: Res. Appl.* 2010;18:573-581.
- [38] Krämer C. S., Zeitler K., Müller T. J. J. First synthesis and electronic properties of (hetero)aryl bridged and directly linked redox active phenothiazinyl dyads and triads. *Tetrahedron Lett.* 2001;42:8619-8624.
- [39] Zhao Y., Zhang Q., Chen K., Gao H., Qi H., Shi X., et al. Triphenothiazinyl triazacoronenes: donor-acceptor molecular graphene exhibiting multiple fluorescence and electrogenerated chemiluminescence emissions. *Journal of Materials Chemistry C.* 2017;5:4293-4301.
- [40] Bard A. J., Faulkner L. R. *Electrochemical Methods: Fundamentals and Applications.* 2nd edn ed. New York: John Wiley and Sons, 2001.
- [41] Lin Y.-D., Chow T. J. Fluorine substituent effect on organic dyes for sensitized solar cells. *J. Photochem. Photobiol. A Chem.* 2012;230:47-54.